Hindawi
Advances in Mathematical Physics
Volume 2019, Article ID 7935067, 9 pages
https://doi.org/10.1155/2019/7935067

Research Article

Numerical Simulation of Ionospheric Disturbance Generated by Ballistic Missile

Jinyuan Zhu,[1] **Hanxian Fang**,[1,2] **Fan Xia**,[1] **Tao Wan**,[1] **and Xiaolin Tan**[1]

[1]*College of Meteorology and Oceanography, National University of Defense Technology, Nanjing 211101, China*
[2]*State Key Laboratory of Space Weather, Chinese Academy of Sciences, Beijing 100190, China*

Correspondence should be addressed to Hanxian Fang; fanghx@hit.edu.cn

Received 23 December 2018; Accepted 11 March 2019; Published 1 April 2019

Academic Editor: André Nicolet

To provide theoretical guidance for the detection of ballistic missiles by skywave over-the-horizon radar, this paper first analyses the best way to detect ballistic missiles based on the rocket detection mechanism. Then using the diffusion model, chemical reaction model, and plasma diffusion model of neutral gas in the ionosphere, this paper studies the distribution of electrons and analyses the disturbance effect on the ionosphere caused by the release of ballistic missile exhaust plume in the ionosphere. Moreover, this paper considers the flight speed of the ballistic missile and the flow of the exhaust plume. Then the effects of different seasons, locations, and time zones on the release are compared. The results show that H_2O can effectively dissipate background electrons to form spindle-shaped holes after release in the ionosphere. The height of the cavity radius corresponds to the peak of electron density of the background ionosphere, and the daytime dissipation is stronger than the nighttime dissipation, dissipation at low latitude is stronger than that at high latitude, and the seasonal difference is not obvious.

1. Introduction

When the Pioneer II was launched in 1959, Booker [1] first observed the existence of ionospheric holes using a drop tester and then repeatedly observed the ionospheric holes generated by the rocket launch. During the launch of the US Saturn V rocket in 1973, the observations from the ATS-3 and ATS-5 geosynchronous satellites showed that due to the large amount of gas released by the rocket (the main components were H_2 and H_2O), the ionosphere forms an ionospheric electron density depletion region with a diameter of 1000 km at a height of 300 km and an ionospheric hole. The electron density in this region is reduced by nearly 50% for a duration of approximately 4 h. This incident interrupted shortwave communication over a large part of the Atlantic [2–4]. As a result of this phenomenon, many countries have used rockets, satellites, and other platforms to carry chemical substances in recent years, consciously releasing these substances into the ionosphere to study the disturbance effects. Mendillo et al. [5, 6] analysed the formation and rapid disappearance of ionospheric holes. It is believed that oxygen ions in the ionosphere undergo rapid ion-atomic exchange reactions with hydrogen and water molecules in the plume to form molecular ions, which are then rapidly combined with electrons in the ionosphere, causing the rapid loss of ionospheric plasma. Mendillo et al. [7] studied the kinetics of neutral gas release in the ionosphere and the physical processes of the expansion, condensation, collision heating, and free diffusion of the release in the near-vacuum environment of the ionosphere, establishing the theoretical basis of releasing chemical substances in the ionosphere. After considering the true ionospheric chemical reaction rate, Anderson and Bernhardt [8] used the model to study the quantitative results of electron loss after releasing H_2 in the equatorial ionosphere and established the disturbed ionospheric evolution model of H_2 point source release. Bernhardt et al. [9] studied several experiments conducted by the Naval Research Laboratory including the Charged Aerosol Release Experiment, the Shuttle Ionospheric Modification with Pulsed Localized Exhaust experiments, and the Shuttle Exhaust Ionospheric Turbulence Experiments.

Table 1: Target characteristics of typical submarine-launched ballistic missiles [12].

Range/km	Engine shutdown height/km	Boost time/s	Re-entry speed/(km/s)	Re-entry angle/degree	flight duration/min
120	80~120	16	1.0	44.7~39.4	2.7
500	80~120	36	20.	44.7~39.4	6.1
1000	80~120	55	2.9	44.7~39.4	8.4
2000	80~120	85	3.9	44.7~39.4	11.8
3000	80~120	122	4.7	44.7~39.4	14.8
10000	200~240	230	7.5	15~35	30

Due to limited data sources, the feasibility and performance of using over-the-horizon radar to detect ballistic missiles cannot be verified. However, its principle and methods are similar to those of detecting a launch vehicle. According to the data, the China Radio Wave Propagation Institute used the 26 MHz HF radar to realize the observation of the active segment of a large launch vehicle [10]. Based on this, this paper starts from the principle and methods of over-the-horizon radar, thus detecting the launch vehicle, and analyses the feasibility of observing ballistic missiles. Combined with the principle of releasing chemical materials to affect the ionosphere, numerical simulations under different constraint conditions are carried out.

2. Skywave Over-the-Horizon Radar Detecting Ballistic Missiles Based on the Rocket Detection Mechanism

The principle and methods of detecting ballistic missile by over-the-horizon radar are roughly the same as those of detecting the launch vehicle; this includes the detection based on the missile itself, the plume, and the artificial ionosphere.

2.1. Projectile-Based Detection. In theory, similar to detecting conventional air targets, over-the-horizon radar can detect ballistic missiles through missiles casing. The missile can be regarded as a type of normal target, with its radar cross section being used to discern size, shape, flight attitude, wavelength, and polarization mode. Combined with the data analysis, if skywave radar only uses the radar cross section to detect the ballistic missile, the effect of the ballistic missile will be not ideal. Usually, the ballistic missile is detected by the strong RCS of the exhaust plume.

2.2. Plume-Based Detection. When launching a missile, the missile generates a powerful plume echo. If high-frequency waves illuminate the plume, the plume will produce a much larger RCS than the missile itself. The plume is a special kind of propagation medium. The plume is a kind of high-temperature and high-speed turbulent airflow emitted by propellant combustion products. The plume is a dense, uneven, and weakly ionized plasma (also known as dust plasma). The plume contains a plurality of chemical constituents, with the electron concentration potentially exceeding 10 /cm3 within a certain plume volume. When the rocket is flying at high altitude, the plume will form a plasma area several times larger than that of the missile. These plasmons provide a good medium for high frequency bands. Therefore, the plume increases the RCS at a high frequency of the rocket.

However, in the airspace below the ionosphere (below 60 km), due to the high atmospheric concentration, even if the rocket exhaust plumes ionize the air molecules, the incident air molecules will immediately be absorbed by the surrounding atmospheric molecules, and effective plasma cannot be formed. Therefore, the radar at this stage can hardly find the rocket's tail plume echo. Under normal circumstances, the rocket is observed at approximately 100 km.

It is known from the previous analysis that skywave over-the-horizon radar can effectively detect the exhaust plume of the ballistic missile only in the ionosphere. This requires that the ballistic missile must fly higher than 60 km before the rocket shuts down.

The working process of US D5 (Trident II), which is a kind of submarine-launched ballistic missile, is as follows [11]: when the countdown of the missile launching programme ends, the operator presses the launch button, the gas launcher of the launching system starts to work, and the missile is fired and launched; the missile relies on the initial velocity to fly forward; when it reaches a certain height, the first-stage engine of the missile is ignited and thrown away after the flameout; then, the second-stage engine is activated and is also thrown away after being extinguished; after the height is above 90 km, the fairing is separated; then, the bullets are released one by one according to the predetermined requirements; and finally, the bullets rush to the target to be attacked.

Some of the main flight parameters of ballistic missiles are shown in Table 1.

Combined with the working process of the US D5 submarine-launched ballistic missile and Table 1, it can be seen that before the shutdown point, the flight height of the US and Russian main ballistic missiles can basically exceed 60 km and enter the ionosphere to meet the skywave radar. Therefore, by using the plume of ballistic missiles, skywave radar can realize the detection of ballistic missiles.

2.3. Artificial Ionospheric Detection. After the launch vehicle enters the ionosphere, the sky-wave over-the-horizon radar may not be able to directly observe the projectile or plume

due to its resolution, etc., but it can also observe the artificial ionospheric hole generated by the plume. During the flight of the missile, a large amount of hydrogen and water molecules in the plume form an area where the total electron content is much lower than the total electron content of the ambient atmospheric background. This area is an artificial ionospheric hole. Skywave radar can estimate the approximate trajectory of rocket targets by detecting these ionospheric holes.

The conditions for detecting ballistic missiles based on artificial ionospheric holes are the same as those based on plume; that is, the flight height of ballistic missiles before the shutdown point is required to enter the ionosphere. Similar to the detection analysis based on plume, if the flight altitude satisfies the condition, then the skywave radar can detect the ballistic missile based on the artificial ionospheric hole. Compared with plume-based detection, artificial ionospheric holes are larger and wider, making it easier for skywave radar to detect targets.

3. Model of the Artificial Ionospheric Hole Generated by Ballistic Missile

At present, theoretical and experimental research on releasing various chemical substances in the ionosphere has made great progress, but a few problems still persist. For example, simulation results predicated on assumptions based on point-source releasing ignore the influence of the speed and attitude of the carrier, the release rate, and the flow rate.

Furthermore, water molecules emitted from the ballistic missile exhaust plume are taken as a test scenario. We consult the modern modelling techniques [9] and consider the effects of the rocket's speed, release rate, and flow rate in the simulation.

3.1. Diffusion Model of Neutral Gas. In the initial stage of the plume's chemical discharge, the material under pressure pushes away the surrounding plasma similar to a snow blower [14, 15]. This process is carried out at supersonic speed, taking a very short amount of time (typically only a few seconds). Then, the pressure difference is sharply reduced. When the material density is compared with the gas density of the background, the releasing material and the surrounding plasma are sufficiently mixed to diffuse into the space. This process takes a long time, with the ion chemical reaction mainly occurring during this stage.

The general equation for neutral gas diffusion is

$$\frac{\partial n_s}{\partial t} + \nabla \bullet \left(v_s n_s\right) = \nabla \bullet \left(D_s \nabla n_s\right) - \sigma n_s, \tag{1}$$

where n_s is the release density, v_s is the initial velocity of the release, D_s is the diffusion coefficient of the release, and σ is the loss coefficient of the release. Considering the initial release as a point source, under the assumption that the ionosphere and the thermal layer are horizontally layered, the motion of the background atmosphere, the thermal diffusion of the neutral molecules, and the expansion process of the chemicals are ignored; the changes in the release density can be approximated by the following formula [16]:

$$\begin{aligned} n_i(r,z,t) = {} & \frac{N_0}{\left(4\pi D_0 t\right)^{3/2}} \exp\left[-(z-z_0)\left(\frac{3}{4H_a} + \frac{1}{2H_i}\right) \right. \\ & - \alpha t - \frac{H_a^2 \left\{1 - \exp\left[-(z-z_0)/(2H_a)\right]\right\}^2}{4D_0 t} \\ & - \frac{r^2 \exp\left[-(z-z_0)/(2H_a)\right]}{4D_0 t} \\ & \left. - \left(\frac{1}{H_a} - \frac{1}{H_i}\right)^2 \frac{D_0 t \exp\left[(z-z_0/(2H_a)\right]}{4} \right], \end{aligned} \tag{2}$$

where z_0 is the height of the release point, N_0 is the total amount of released molecules, $H_\alpha = kT/(m_a g)$ is the atmospheric elevation, $H_i = kT/(m_s g)$ is the elevation of the released gas, k is the Boltzmann constant, T is the background gas temperature, m_a, m_s are the average molecular weight of the atmosphere and the molecular weight of the released gas, g is the acceleration of gravity, and αt is the loss item caused by the chemical reaction.

Suppose the background atmosphere consists of O, O_2, and N_2. Taking the chemical substance H_2O as an example, the diffusion coefficient at the release point can be expressed as [17]

$$\begin{aligned} D_0 = {} & \left(\frac{n_O}{8.46 \times 10^{17} T^{0.5}} + \frac{n_{N_2}}{2.04 \times 10^{17} T^{0.623}} \right. \\ & \left. + \frac{n_{O_2}}{2.02 \times 10^{17} T^{0.632}} \right)^{-1} cm^2 \bullet s^{-1}, \end{aligned} \tag{3}$$

where n_O, n_{N_2}, and n_{O_2} represent the number density of O, O_2, and N_2, respectively.

3.2. Chemical Reaction Process. Gas molecules of H_2O can reduce the electron density in the flight region. This is mainly because the composite coefficient of the O^+ and electrons in the ionosphere is about $10^{-12} cm^3 \bullet s^{-1}$, and neutral gases allow for easy conversion of atomic O^+ into molecular particles, with the composite coefficient generally reaching $10^{-7} cm^3 \bullet s^{-1}$ or even larger [18]. Therefore, the electron density of the ionosphere is likely to be low, resulting in artificial ionospheric holes.

The main chemical reaction processes in ionospheric plasma are shown in Table 2, where k_1 and k_2 are chemical reaction coefficients and T_e is the electron temperature. The electron density reduction is

$$\Delta n_e = k_2 \left(k_1 n_{H_2O} n_O + \Delta t\right) n_e \Delta t. \tag{4}$$

3.3. Plasma Diffusion. The change in electron density in the chemical release region destroys the density distribution structure and the dynamic balance of the original charged particles. This is due to the interactions among the electric field, magnetic field, ion and electron density gradient, collisions in ionosphere disturbance zone, neutral wind, etc.

Table 2: Reactions stimulated by H_2O release in the ionosphere [13].

Num.	Reaction equation	Reaction coefficient/$cm^3 \bullet s^{-1}$
1	$H_2O + O^+ \xrightarrow{k_1} H_2O^+ + O + 1.01eV$	$k_1 = 3.2 \times 10^{-9}$
2	$H_2O^+ + e^- \xrightarrow{k_2} H + OH^* + 7.45eV$	$k_2 = 6.5 \times 10^{-7} \left(300/T_e\right)^{0.5}$

The detailed stress situation is complex, since the plasma will drift; in the F zone, we only consider the maximum force, that is, the role of the magnetic field.

The plasma continuity equation is

$$\frac{\partial n_p}{\partial t} = -\nabla \bullet \left(n_p v_p\right) + P - L, \tag{5}$$

where n_p is the ion or electron density; P and L are the production and loss items of the charged particles, respectively; v_p is the drift velocity of the plasma along the magnetic fields, and the calculation expression is

$$v_p = -\mathrm{D}\left[\frac{\partial \ln n_p T_p}{\partial s} + \frac{\sin I}{H_p}\right] + v_D, \tag{6}$$

where D is the plasma diffusion coefficient, T_p is the plasma temperature, and I is the magnetic dip. Since we assume that the plasma only drifts along the magnetic field, the continuity equation is rewritten as

$$\begin{aligned}\frac{\partial n_p}{\partial t} = -\Bigg[&\sin I \frac{\partial \left(n_p v_p\right)}{\partial z} + \cos I \frac{\partial \left(n_p v_p\right)}{\partial x} \\ &+ \sin \varphi \frac{\partial \left(n_p v_p\right)}{\partial y}\Bigg] + P - L,\end{aligned} \tag{7}$$

where φ is magnetic deflection.

3.4. Release Rate. At the moment of plume injection, the release is quickly ejected under the pressure. According to fluid mechanics, the release rate can be expressed as

$$v_e = \sqrt{\frac{2kT}{m_s}}. \tag{8}$$

The speed of ballistic missiles mainly affects the simulation results by affecting the initial velocity. Since the process of plume injection is the process of chemical release, the initial velocity only needs to consider the speed of ballistic missiles. Therefore, the speed of ballistic missiles is expressed as

$$v_0 = v_e + v_{rocket}. \tag{9}$$

After the release, due to the effect of inertia, the release cloud will continue to move a certain distance; under the resistance of the background atmosphere, the velocity of the release cloud slowly decreases until it is relatively stationary with the background. During the movement of the cloud, the momentum equation is satisfied. After release, the released cloud pressure quickly drops to the background atmosphere level; thus, the release cloud pressure can be neglected, and the background gas is considered to be stationary. Regardless of the change in the velocity of the release cloud, the speed of motion can be simply expressed as

$$v_c = v_0 \bullet \exp\left(-\nu t\right). \tag{10}$$

According to the dynamic analysis of the release cloud, upon solving the diffusion equation of the release, the release of the release cloud is no longer regarded as a simple point source diffusion, but as several point sources of different initial positions, different release times, and different release amounts in order to obtain an emission density distribution.

3.5. Mathematical Model Design. According to the release parameters and the physicochemical processes of neutral particles in the ionosphere, the simulation model of the release is established by solving the release diffusion process and the plasma diffusion equation. The design flow of the model algorithm is shown in Figure 1. The effect simulation process is performed in the following four steps.

(a) Release parameters are set according to the specific conditions of the test, including release parameters and rocket flight parameters.

(b) The release process is solved to obtain the release density distribution.

(c) The electron density distribution is calculated according to the chemical reaction and the plasma diffusion process.

(d) The remaining emissions of the chemical reaction continue to diffuse, and steps 2 to 3 are repeatedly performed to calculate the plasma density at the next moment, thereby obtaining the ionization cloud density distribution at any time; that is, the space is the ionization cloud density distribution.

4. Numerical Simulation Results

4.1. Simulation Parameter Settings. The background ionospheric parameters and neutral atmospheric parameters are obtained from the empirical models IRI-2016 and NRLMSISE-00, respectively. The location of the simulation test was in the mid-latitude city of Nanjing (119° east longitude, 32° north latitude), and the time was LT 12:00 on January 1, 2018. First, the neutral atmosphere and ionospheric parameters of the release region are obtained by the empirical mode, and the spatial distribution of the H_2O molecules ejected in the plume is obtained by the diffusion equation. Then, the conditions of the ion chemical reaction equation and

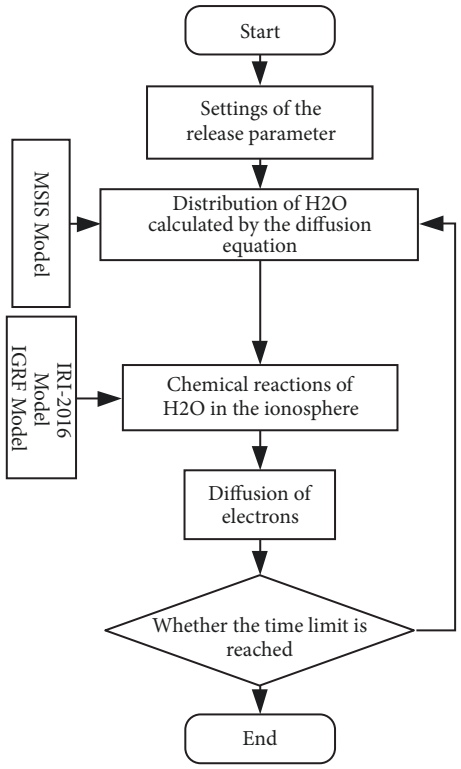

Figure 1: Flow chart of ionosphere disturbance by ballistic missile exhaust plume.

the quasi-neutral characteristics of the plasma are obtained. Thus, the electron density change in the release region can be determined. Then, the time step is further pushed forward, and the above cycle is repeated to obtain the electron density at the next moment, with the time step being taken as 1.0 s.

4.2. Particle Density Distribution under the Release of Moving Targets. Assuming that the ballistic missile's speed is approximately 10 km/s and that 2240 mol of H_2O is released every 2 s from 200 km to 360 km in the vertical direction, that is, 2240 mol of H_2O are released every 20 km in the vertical upward path, then the density distribution of electrons after 100 s is shown in Figure 2.

It can be seen from the figure that H_2O produced by ballistic missile combustion can form a large range of electron density voids in the ionosphere in a short time. The section of the ionospheric void at 100 s is approximately a spindle type. At the peak height of the ionospheric electron density, electrons are mostly dissipated and the range of voids is the widest. The maximum radius of the cavity is approximately 40 km, and the minimum is 20 km.

4.3. Comparison of Day and Night Launches. Figure 3 shows the background ionospheric electron concentration profiles for LT 12:00 and LT 00:00 on January 1, 2018, respectively. It can be seen from the figure that the electron concentration at

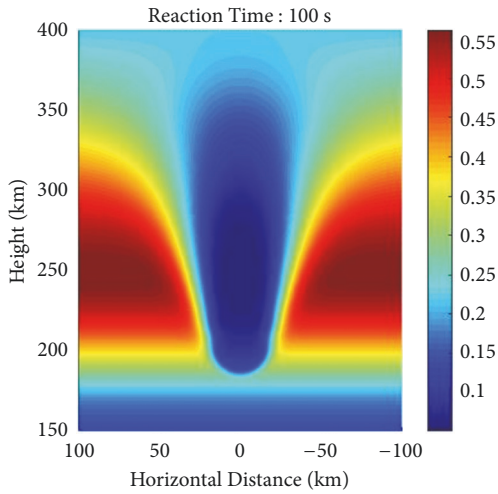

Figure 2: Electron density profile of H_2O released from the ionosphere in the ballistic missile exhaust plume in Nanjing in winter.

night is significantly lower than that during the day, and the peak of electron density in the range of 150-400 km is only 1/7 that of the daytime. In addition, the peak height of the nighttime electron density is approximately 320 km, and the peak height of the daytime electron density is approximately 250 km.

Figure 4 shows the effect of the release of the same quality of chemicals for 100 s during both the day and night. It is simulated that the ballistic missile exhaust plume releases 2240 mol of H_2O every 2 s from 200 km to 360 km, and the electron density profile is shown in Figure 4. It can be seen that since the electron concentration at night is inherently low, the ionospheric voids generated are not obvious.

Through the comparison of daytime and nighttime release effects, it can be clearly seen that the daytime electron dissipation is much larger than the nighttime electron dissipation. This finding indicates that the disturbance during the day is larger than that during the night. This is mainly because the physical characteristics of the nighttime ionosphere are much smaller than those in daytime conditions, the rate of the chemical reaction will be slower at night, and the peak height of electron density at night is higher than that during the day. The higher the chemical content is, the faster the level of diffusion, which results in more unfavourable conditions for the reaction of chemical substances and electrons, meaning that electron density dissipation is not as good during the nighttime environment.

4.4. Comparison of Launching Ballistic Missiles in Different Seasons. Figure 5 shows the background ionospheric electron density profile for the Nanjing area on July 1, 2017. In comparison with the graph of January 1, 2018, it is found that both the maximum electron concentration and the peak height are similar.

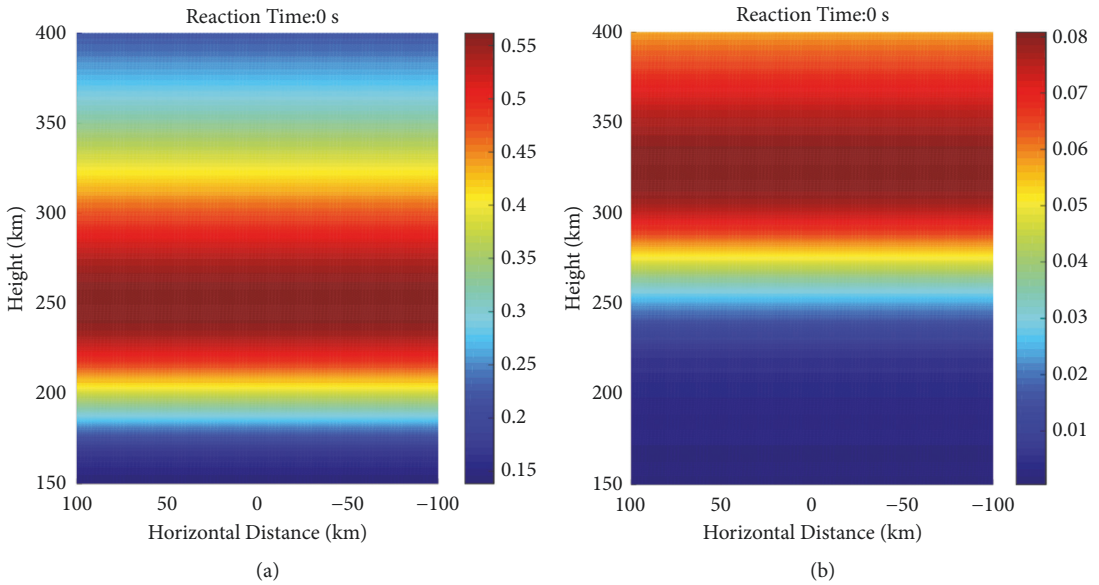

FIGURE 3: (a) Background ionospheric electron concentration profile during the day; (b) background ionospheric electron concentration profile during the night.

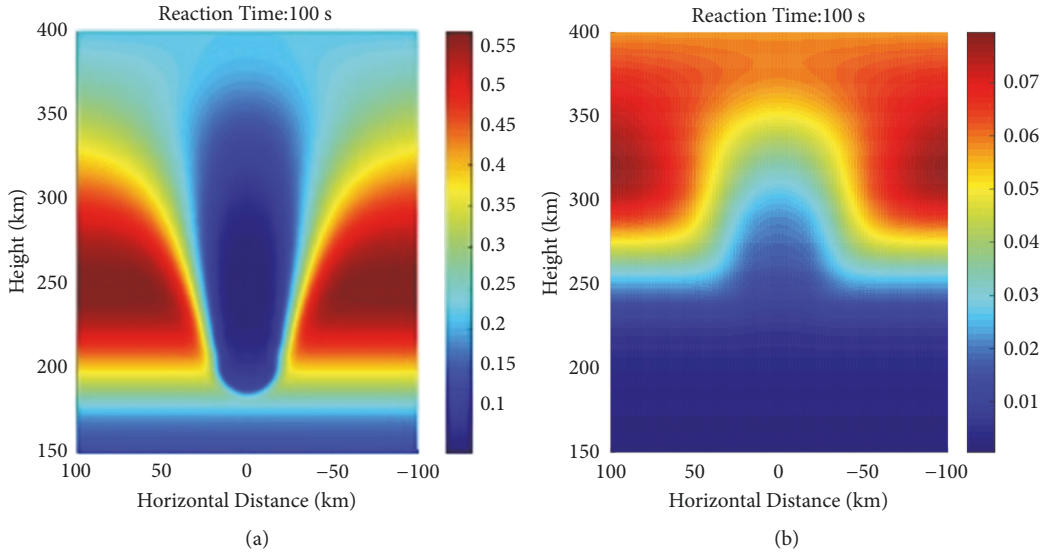

FIGURE 4: (a) Electron density profile of H_2O released from the ionosphere during the day; (b) electron density profile of H_2O released from the ionosphere during the night.

The launch of ballistic missiles was simulated in the Nanjing area in the summer, resulting in the release of the water molecules in the plume into the ionosphere at LT 12:00, releasing the same height. As seen from Figure 6, the resulting ionospheric void is still the spindle type, the maximum cavity radius reaches approximately 40 km, and the minimum cavity radius is 20 km. The difference between the simulation and the winter is not obvious.

4.5. Comparison of Launching Ballistic Missiles at Different Locations. Consider ballistic missile launches at different locations. Two different locations were selected, Yinchuan, Ningxia (106° east longitude, 37° north latitude) and Haikou, Hainan (110° east longitude, 19° north latitude). The latitude and longitude of these two locations are quite different, which allows us to see the effect of spatial differences. Figure 7 shows the electron density of the background ionosphere in Yinchuan and Haikou. It can be clearly seen from the figure that the peak of the electron concentration in low latitudes is greater than that in high latitudes. This observation occurs more than twice. Moreover, the peak height of the electron concentration in low latitudes is greater than that in high latitudes.

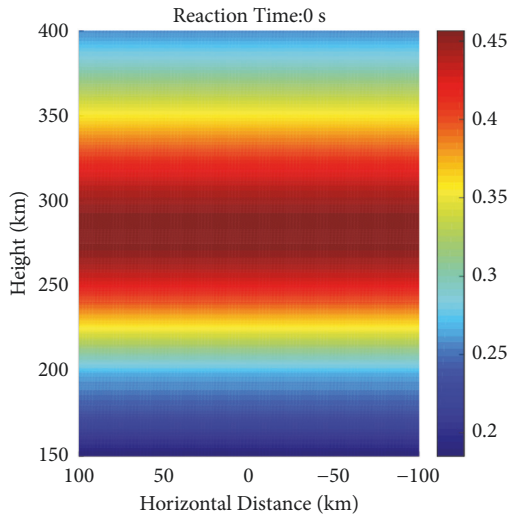

Figure 5: Background ionospheric electron concentration profile in the Nanjing area in summer.

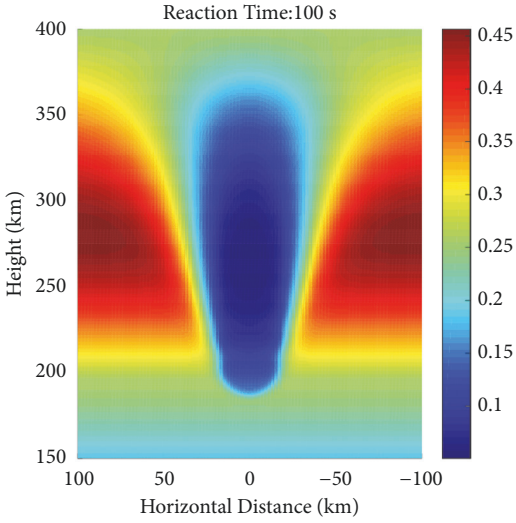

Figure 6: Electron density profile of H_2O released from the ionosphere in the simulated exhaust plume in Nanjing in summer.

Similarly, the condition of ballistic missile exhaust plume releasing 2240 mol of H_2O every 2 s from 200 km to 360 km was simulated, and then the effects in two places of releasing at 100 s were compared.

Figure 8 shows that after 100 s of release, the electron density dissipation in the low latitudes is more pronounced, upon observing the peak ion density of the background ionosphere. This may be because the parameters in the low latitude area are large, which is more conducive to the collision between particles, allowing for more intense chemical reactions. At the same time, since the reaction times are both 100 s, the range of ionospheric holes generated is not very different.

5. Conclusion

According to the analysis of the mechanism of over-the-horizon radar in detecting rockets in the existing data, the feasibility of using an ionospheric hole formed by the plume to detect the ballistic missile is demonstrated. Five groups of data were selected with varying parameters, such as day/night cycle, season, and region (total of 3). Under the assumption that the background ionosphere level was uniform, the simulation of the ionospheric release of the ballistic missile exhaust plume's chemical substance H_2O was performed. The response process and the effects of various forms of release were analysed. By comparing the differences in chemical substances released at different times, seasons, and varying latitudes and longitudes, the following conclusions are obtained through comprehensive analysis.

(a) The chemical substance H_2O in the ballistic missile exhaust plume can diffuse on a large spatial scale after being released into the ionosphere, and it can effectively react with the background electrons. The release centre can cause the background electron density to dissipate in a short time, forming electron density voids. The plume forms an approximately elliptical distribution on the vertical section.

(b) The electron density cavity profile formed by the plume shows that the disturbance effects of different heights are different. The height of the cavity radius corresponds to the peak of electron density of the background ionosphere. The dissipation of the daytime release is much larger than the nighttime electron dissipation effect. The seasonal difference is not obvious. The dissipation in lower latitudes is greater than that in higher latitude.

(c) It is feasible that over-the-horizon radar uses the electron density cavity formed by the plume to detect the presence of a ballistic missile. This becomes apparent when observing a ray passing through the hollow area.

Although the above conclusions take the speed of the ballistic missile and the flow of the released matter into account, they are based on the assumptions and approximations of the ionospheric level uniformity while ignoring the neutral wind field. The neutral chemical diffusion model only considers the two-dimensional direction, and the flight of ballistic missiles only considers the vertical direction. Moreover, the background parameters are derived from the empirical mode, which is still different from the real physical environment; thus, the simulation accuracy needs to be studied further.

Data Availability

The ionospheric initial data used to support the findings of this study are available from the corresponding author upon request.

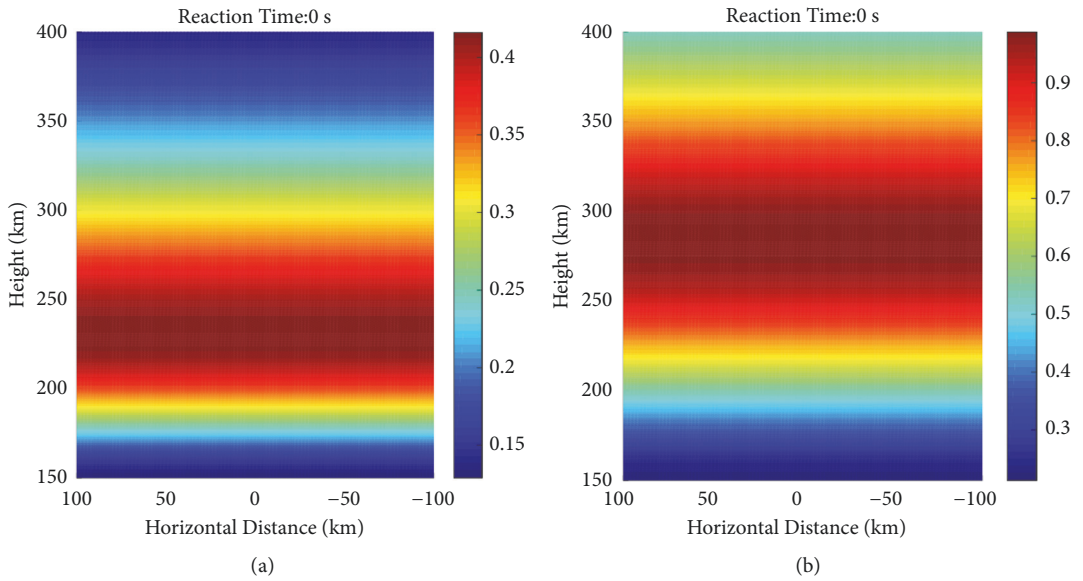

FIGURE 7: (a) Background ionospheric electron concentration profile in Yinchuan; (b) background ionospheric electron concentration profile in Haikou.

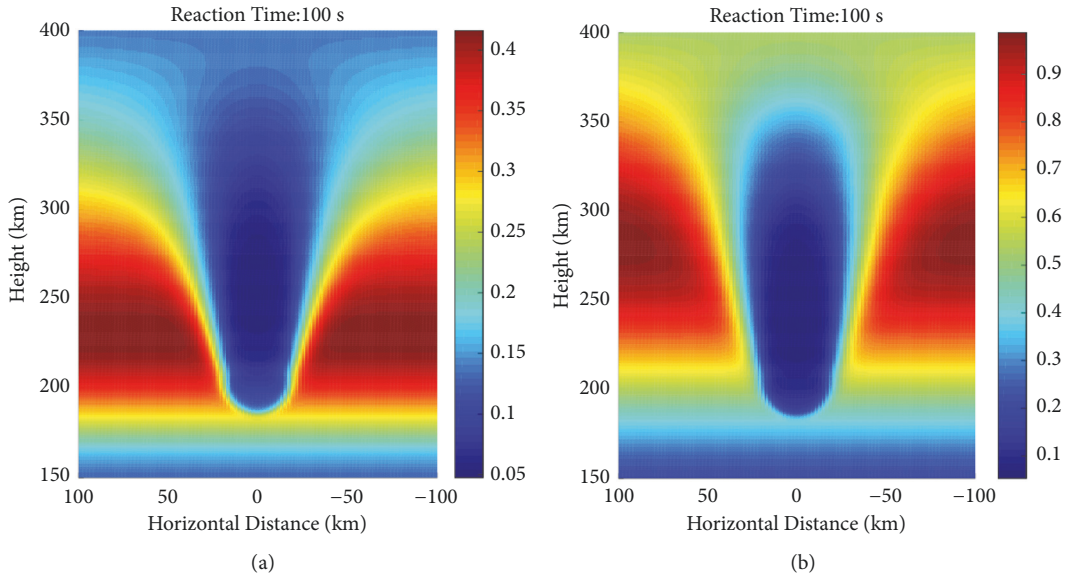

FIGURE 8: (a) Electron density profiles of H_2O released from the ionosphere in simulated plumes in Yinchuan; (b) electron density profiles of H_2O released from the ionosphere in simulated plumes in Haikou.

Conflicts of Interest

The authors declare that there are no conflicts of interest regarding the publication of this paper.

Acknowledgments

The research and publication of our article are funded by the National Natural Science Foundation of China (no. 40505005).

References

[1] H. G. Booker, " A local reduction of *F* -region ionization due to missile transit ," *Journal of Geophysical Research: Atmospheres*, vol. 66, no. 4, pp. 1073–1079, 1961.

[2] M. Mendillo, G. S. Hawkins, and J. A. Klobuchar, "A Large-Scale Hole in the Ionosphere Caused by the Launch of Skylab," *Science*, vol. 187, no. 4174, pp. 343–346, 1975.

[3] M. Mendillo, G. S. Hawkins, and J. A. Klobuchar, " A sudden vanishing of the ionospheric *F* region due to the launch of

Skylab ," *Journal of Geophysical Research: Atmospheres*, vol. 80, no. 16, pp. 2217–2228, 1975.

[4] J. Zinn, C. D. Sutherland, S. N. Stone, L. M. Duncan, and R. Behnke, "Ionospheric effects of rocket exhaust products—heao-c, skylab," *Journal of Atmospheric and Solar-Terrestrial Physics*, vol. 44, no. 12, pp. 1143–1171, 1982.

[5] M. Mendillo, M. Jeffrey, and J. M. Forbes, "Artificially created holes in the ionosphere," *Journal of Geophysical Research*, vol. 83, no. A1, pp. 151–163, 1978.

[6] M. Mendillo and J. M. Forbes, "Theory and observation of a dynamically evolving negative ion plasma," *Journal of Geophysical Research: Atmospheres*, vol. 87, no. A10, p. 8273, 1982.

[7] M. Mendillo, S. Smith et al., "Man-made space weather," *Space Weather Journal*, vol. 6, no. 9, 2008.

[8] D. N. Anderson and P. A. Bernhardt, "Modeling the effects of an H_2 gas release on the equatorial ionosphere," *Journal of Geophysical Research*, vol. 83, no. A10, pp. 4777–4790, 1978.

[9] P. A. Bernhardt, J. O. Ballenthin, J. L. Baumgardner et al., "Ground and Space-Based Measurement of Rocket Engine Burns in the Ionosphere," *IEEE Transactions on Plasma Sciences*, vol. 40, no. 5, pp. 1267–1286, 2012.

[10] W. Y. Zhou and P. N. Jiao, *Over-the-horizon Radar Technology*, Electronic Industry Press, Beijing, China, 2008.

[11] Z. N. Han, *Analysis of Famous Foreign Missiles*, National Defense Industry Press, Beijing, 2013.

[12] W. N. Lu, *Ballistic Missile Attack and Defense Confrontation Technology*, China Aerospace Press, Beijing, China, 2007.

[13] P. A. Bernhardt, "A critical comparison of ionospheric depletion chemicals," *Journal of Geophysical Research: Atmospheres*, vol. 92, no. A5, p. 4617, 1987.

[14] Y. G. Hu, Z. Y. Zhao, and Y. N. Zhang, "Study on ionospheric release effects of several typical chemicals," *Acta Phys. Sin*, vol. 59, no. 11, pp. 8293–8303, 2010.

[15] R. W. Schunk and E. P. Szuszczewicz, "Plasma expansion characteristics of ionized clouds in the ionosphere: Macroscopic formulation," *Journal of Geophysical Research: Space Physics*, vol. 96, no. A2, pp. 1337–1349, 1991.

[16] N. A. Gatsonis and D. E. Hastings, "A three-dimensional model and initial time numerical simulation for an artificial plasma cloud in the ionosphere," *Journal of Geophysical Research: Atmospheres*, vol. 96, no. A5, p. 7623, 1991.

[17] M. Mendillo, J. Semeter, and J. Noto, "Finite element simulation (FES): A computer modeling technique for studies of chemical modification of the ionosphere," *Advances in Space Research*, vol. 13, no. 10, pp. 55–64, 1993.

[18] O. P. Kolomiitsev, Y. Y. Ruzhin, and L. B. Egorov, "Ionosphere plasma holes-modeling and diagnostic," *Phys. Chem. Earth*, vol. 24, no. 4, pp. 393–399, 1999.